Chapter 9

C-terminal truncation of α-Synuclein protein (1-99 and 1-108) and its subsequent effect on membrane protein interaction

C-terminal truncation of α-Synuclein protein (1-99 and 1-108) and its subsequent effect on membrane protein interaction

9.1. Abstract:

Accelerated progression rates in PD have been linked to CTD truncations of monomeric α-Syn, which have been suggested to increase amyloid aggregation *in vivo* and *in vitro*. In the brain of PD patients, CTD truncated α-Syn was found to have lower cell viability and tends to increase in the formation of fibrils. The CTD of α-Syn acts as a guard for regulating the normal functioning of α-Syn. The absence of the CTD may allow the N-terminal of α-Syn to interact with the membrane thereby affecting the normal functioning of α-Syn, and all of which will affect the etiology of PD. In this study, the conformational dynamics of CTD truncated α-Syn (1-99 and 1-108) monomers and their effect on the protein-membrane interactions were demonstrated using the all-atom MD Simulation method. From the MD analyses, it was noticed that among the two truncated monomers, α-Syn (1-108) was found to be more stable, shows rigidness at the N-terminal region, and contains a significant number of intermolecular hydrogen bonds between the NAC region and membrane, and lesser number of extended strands. Further, the bending angle in the N-terminal domain was found to be lesser in the α-Syn (1-108) in comparison with the α-Syn (1-99). Our findings suggest that the truncation on the CTD of α-Syn affects its interaction with the membrane and subsequently has an impact on the aggregation.

9.2. Introduction:

The development of intracellular aggregates of fibrils of the intrinsically disordered protein α-Syn is the main characteristic feature of PD that distinguishes it from other neurodegenerative disorders [117, 519, 548]. The involvement of fibrillation of α-Syn in neuronal cell death in PD is now well known [549, 550]. The N-terminal region (residues 1–60), which is primarily involved in membrane binding [551], the NAC domain (residues 61–95), which is essential for amyloid formation [552], and the highly charged C-terminal region (residues 96–140), which is known to interact with polyamines, metal ions, and cellular protein [553]. The remarkable capacity of truncated CTD α-Syn to aggregate and convert into pathological fibrils has led to the detection of many types of truncated CTD α-Syn in both normal and PD brains [554-558]. *In vitro*, truncated CTD α-Syn speeds up the development of oligomers and fibrils in comparison to full-length protein [174, 559-564]. When full-length α-Syn and truncated CTD α-Syn are co-expressed, full-length α-Syn pathologically accumulates more quickly [175,176,

565, 566]. Up to residues 85–90, when the NAC domain starts, deletion of C-terminal residues speeds aggregation [567, 568]. Because the NAC region functions as the core of amyloid fibrils, further truncation reduces the chances of aggregation [138, 567, 569]. Since truncated CTD α-Syn is more toxic than full-length α-Syn, cells expressing it are more susceptible to oxidative stress [564, 570-572]. According to studies, the charges in the positive N-terminal and negative C-terminal regions helps to partly protect the NAC domain [573]. However, α-Syn has dynamic conformations with a significant degree of compactness that are stabilized by long-range interactions [573]. Due to the impact of electrostatic and hydrophobic contacts that may hinder aggregation, these interactions take place between the NAC area and the C-terminal region as well as between the N-terminal and C-terminal regions [573]. Additionally, it has been stated that the membrane-sensor area is likely to include the NAC domain, which is important for α-Syn aggregation propensity and also has functional importance [140, 552, 574]. The NAC domain may control the partition between the bound and free states of the membrane in the synaptic terminal as well as define the amount of α-Syn with lipid membranes [138,575, 576, 577, 578]. PD is characterized by the presence of amyloid deposits made of misfolded proteins in specific regions of the nervous system. A key feature of PD is a conformational shift of native proteins that causes the aggregation and production of insoluble amyloid fibrils, despite the fact the processes behind neurodegeneration are still poorly understood. The main pathological marker of PD is the presence of LB. These LB in the brain of PD patients contain amyloid fibrils with a cross-β structure. The most amyloidogenic regions of a protein, applied to α-Syn confirmed a high intrinsic aggregation propensity for the NAC region, with the highest propensity for region 69–79 [579]. Also, in the diseased mutants amyloid formation plays a significant role in α-Syn toxicity [580]. In fact, previous studies have shown that α-Syn occurs *in vivo* in a state of equilibrium between the membrane-bound and cytosolic forms, with membrane partition being strictly controlled [18]. During aggregation, the α-Syn and membrane interactions emphasize the significance of the interplay between different functional modes of α-Syn and its aggregation mechanism, resulting in PD [28]. Compared to the cytosolic form, the membrane-bound form has a greater propensity to aggregate, and the aggregates created within the membrane function as "seeds" to quicken the aggregation of the free cytosolic α-Syn [29]. Furthermore, changes in the lipid composition or chemical modification of membrane lipids may also result in structural modifications to the membrane that facilitate aggregation. One such structural modification includes oxidative modifications in lipids and/or the protein that was found to play a role in the aggregation in the membrane. Also, a common phenomenon is that in aged brains there is increase in oxidative damage to the

lipid membrane. Given its greater tendency for aggregation and seeding capacity, the membrane-bound form may represent a nucleating species. Membrane lipid oxidation may encourage α-Syn aggregation by either creating an environment that is favorable for α-Syn self-assembly or by causing oxidative alterations of α-Syn that alter the protein's structure and increase its susceptibility to aggregation.

In this study, the effect of CTD truncation (1-99 and 1-108) of α-Syn on the membrane association was demonstrated using all-atom MD Simulation. The CTD truncation (1-99) of α-Syn releases the N-terminal domain that enhances its association with membrane and disrupts the long range interaction between the N-terminal and C-terminal responsible for maintaining the conformation of α-Syn [173]. Also, the inhibition of long-range interaction between the N-terminal and NAC region by CTD truncation (1-99) results in the exposure of the NAC region that enhances fibrillation of αSyn [581]. The CTD truncation (1−108) αSyn fibrils consist of strongly bent β-sheets with greater solvent dissolving factor as compared to untruncated α-Syn [568]. The form and physical-chemical characteristics of amyloid fibrils are influenced by variations in the fold of monomers (1-108), which might lead to variations in their cytotoxicity [582]. Our study presents the intermolecular Hydrogen bond analysis of truncated CTD α-Syn (1-99 and 1-108) that indicates the lower interaction between the regions of more truncated α-Syn (1-99) and lipid membrane. From our findings, the truncated CTD can be suggested to modulate the α-Syn aggregation by interfering with the binding of the α-Syn protein to the membrane and providing support for the pathogenic function of CTD truncation in PD development.

9.3. Materials and Methods:

9.3.1. Preparation of C-terminal truncated α-Synuclein monomers:

The 3-D structure of α-Syn (PDB ID: 1XQ8) was retrieved from the Protein Data Bank [457] and was used to generate the model structure of the two truncated counterparts of the protein: C-terminal truncation (1-99) α-Syn and (1-108) α-Syn (**Figure 9.1**). This structure was created by truncating the residues (1-99 and 1-108) of the CTD using the CHIMERA visualization software [306].

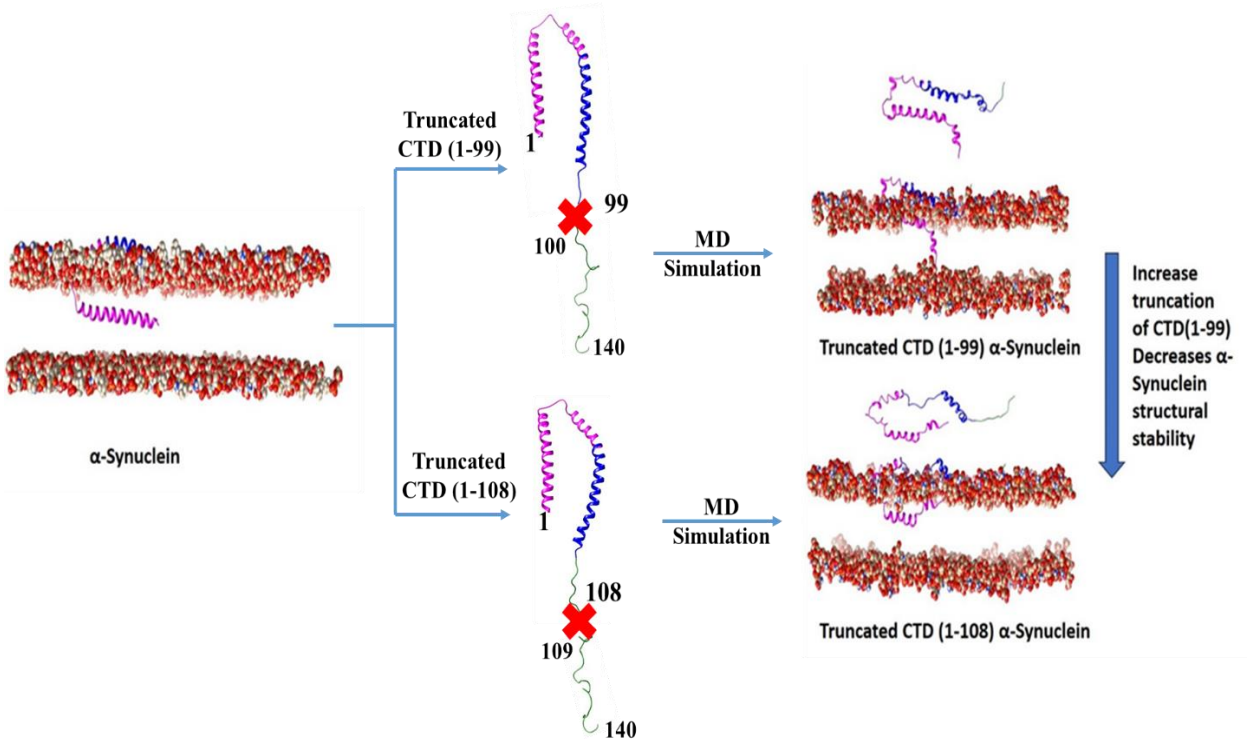

Figure 9.1. *Truncation of CTD of α-Syn (1-99 and 1-108) followed by MD simulation*

9.3.2. Preparation of Simulation setup for truncated C-terminal domain of α-Synuclein:

To initiate the assembly of the membrane bilayer and truncated CTD α-Syn (1-99 and 1-108), the structures were uploaded to the CHARMM GUI server [220]. The MD simulation setup module was performed as mentioned in section **4.3.2.**

9.3.3. MD simulation analysis:

Structural analysis of MD simulation for the truncated CTD α-Syn (1-99 and 1-108) was performed using the CPPTRAJ module [305] of AmberTools 18. To assess the adopted simulation protocol, we have analyzed APL and EDP analysis. The backbone RMSD of Cα atoms was analyzed to study the stability and convergence of membrane-bound truncated CTD α-Syn (1-99 and 1-108). To check the flexible and rigid regions of membrane-bound truncated CTD α-Syn (1-99 and 1-108), RMSF were calculated from their corresponding trajectories obtained during MD simulation and plotted with respect to the residue index. The distance analysis between the N-terminal and truncated CTD α-Syn (1-99 and 1-108) was plotted. The secondary structural analysis of truncated CTD α-Syn (1-99 and 1-108) was calculated using the Kabsch and Sander algorithm [295], and the percentage of secondary structure was calculated using SOPMA servers [286]. Intermolecular hydrogen bond analysis is used to

analyze the proximity between the lipid bilayer and NAC regions of truncated α-Syn (1-99 and 1-108). Using the HELANAL server [285], the average number of helix per turn, helix length, and bending angle of α-Syn helix were calculated. The list of residue-residue contacts and the distance between the N-terminal, NAC region, and C-terminal of the shortened CTD α-Syn (1-99) and (1-108) monomers interface were assessed using the ESBRI server [259]. The MD analyses were plotted using the xmgrace tool.

9.3.4. Principal Component Analysis (PCA) followed by free energy landscape of MD trajectories:

PCA is a widely used multivariate statistical method employed to effectively reduce the dimensionality required for describing protein dynamics [303, 304]. This technique involves a decomposition process that systematically filters observed motions based on their spatial scales, starting from the largest and progressing to the smallest. To represent the internal dynamics of a protein, PCA must be applied to Cartesian coordinates that define the locations of atoms [510]. This requires an alignment step before building the C-matrix. The stage of structural alignment necessitates a global rotation in addition to the center of masses being in perfect alignment with one another to achieve the best possible alignment of the structures. The PCA analysis was performed as mentioned in section **8a.3.6**.

9.4. Results and Discussions:

9.4.1. Area per lipid analysis of truncated CTD α-Synuclein monomers:

The overall amount of lipids in the entire system is then divided by the surface area of the bio-membrane to determine its density. Average APL surface was shown to be a criterion for choosing equilibrium configurations in the DOPE/DOPS/DOPC simulation system of truncated CTD α-Syn (1-99 and 1-108). It was able to calculate the surface APL layer by dividing the entire surface area of the simulated box by the total number of lipids in a single leaflet. The surface APL layer was calculated by dividing the entire surface area of the simulated box by the total number of lipids in a single leaflet. **Figure 9.2** shows the time-dependent APL of truncated CTD α-Syn (1-99 and 1-108) for the DOPE/DOPS/DOPC lipid bilayer respectively. From a 100 ns trajectory, the APL for the DOPE/DOPS/DOPC system was determined for truncated CTD α-Syn (1-99 and 1-108) to be 65.32 Å and 66.19 Å for the upper leaflet and 67.83 Å and 68.74 Å for the lower leaflet.

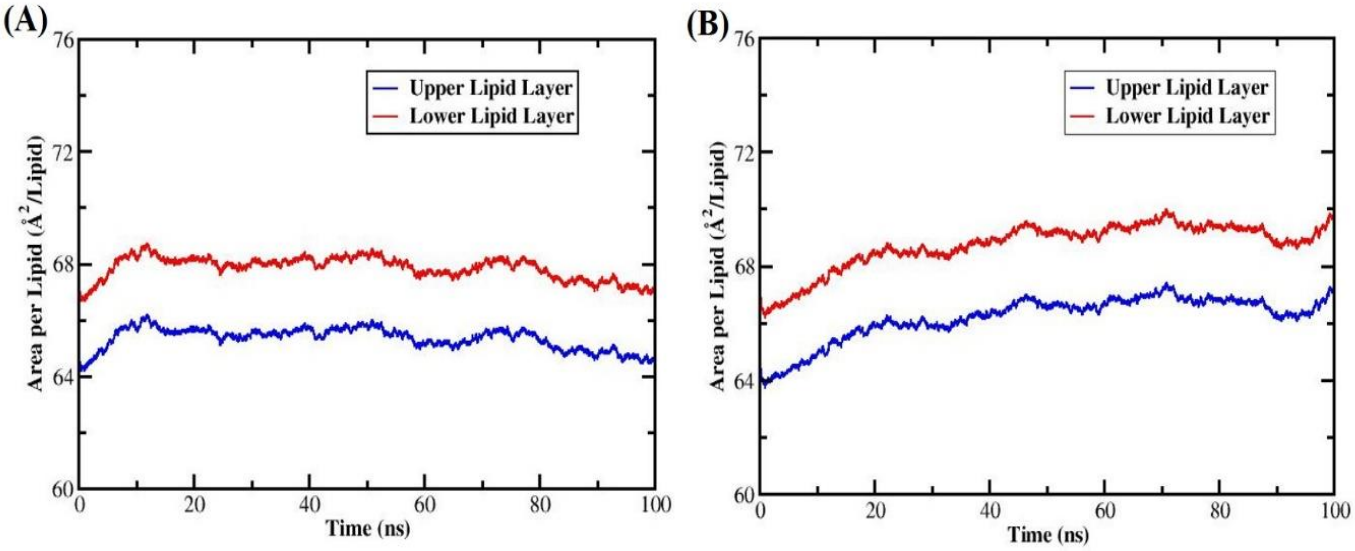

Figure 9.2. *Area per lipid analysis of truncated CTD α-Syn (1-99 and 1-108) from the MD simulation trajectories*

9.4.2. Electron Density Profile Analysis of truncated CTD α-Synuclein monomers:

To calculate the EDP, it was assumed that each atom's center partial charge was subtracted from the electron charge, which was equal to the atomic number. The decomposition of the EDP into several groups, including water, choline (CHOL), phosphate (PO4), serine, ethanolamine, and oleoyl groups, is shown in **Figure 9.3**. There are three unique zones that may be seen when all-atom densities are used, according to the density profiles of DOPE, DOPS, and DOPC. The assembly of the lipids in a 5:3:2 ratio on both lipid monolayers was what defined the mixed lipid bilayer of DOPE, DOPS, and DOPC. According to the EDP for the molecular components of the truncated CTD α-Syn (1-99 and 1-108) systems as shown in **Figure 9.3**, the EDP were found to be constant on both sides of the membrane at 20 Å for all simulated trajectories, suggesting that the simulations were well-balanced. The positioning of molecules and the nature of their chemical components inside a bilayer are typically described using EDPs. **Figure 9.4** shows the EDP profiles for the N-helix and Turn regions of the truncated CTD α-Syn (1-99 and 1-108) systems. The N-helix region of the truncated CTD α-Syn (1-99 and 1-108) systems was discovered to reside immediately below the lipid head group/water interface, allowing the hydrophobic face of the protein to connect with the lipid's hydrophobic core and the hydrophilic face to interact with the lipid's polar region and water. The binding environment of the truncated CTD α-Syn (1-99 and 1-108) in the bilayer is substantially changed since Helix-N of truncated CTD α-Syn (1-99) ends up at a deeper depth

of 8 Å underneath the lipid head group phosphates than the truncated CTD α-Syn (1-108). The turn region of truncated CTD α-Syn (1-99) is more exposed to the water surface as it submerged 5 Å below the bilayer center. In **Figure 9.4(B)** of truncated CTD α-Syn (1-108), the turn region is tunnelling through the bilayer at a depth of 12 Å and is considered to be correspondingly submerged more at a depth from the bilayer center (Z=0).

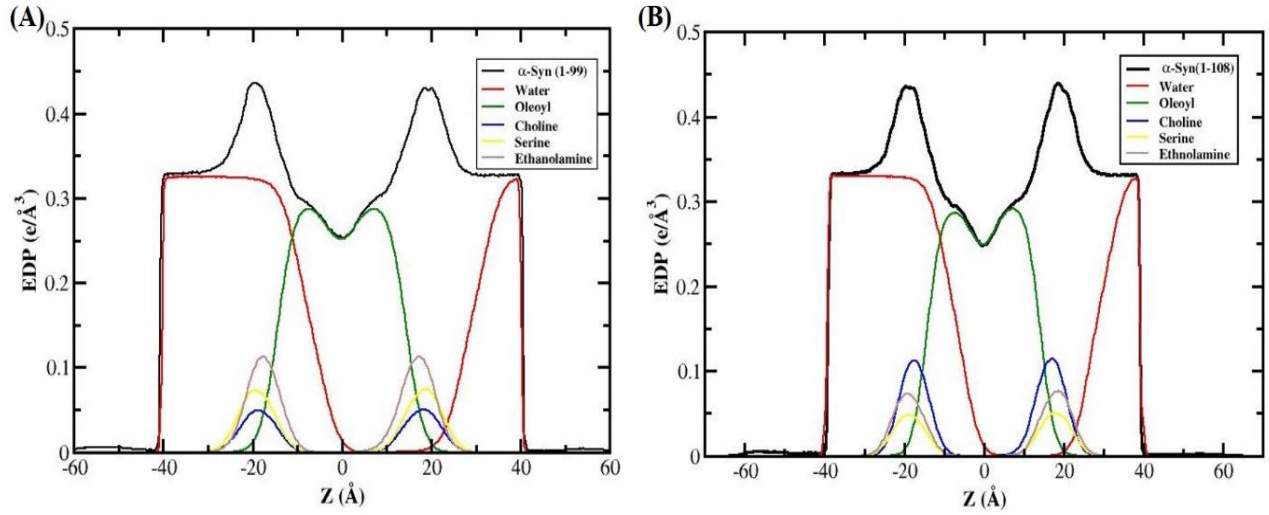

***Figure 9.3**. Electron Density Profile analysis of each component of truncated CTD α-Syn (A) (1-99) and (B) (1-108) from the MD simulation trajectories of 100 ns*

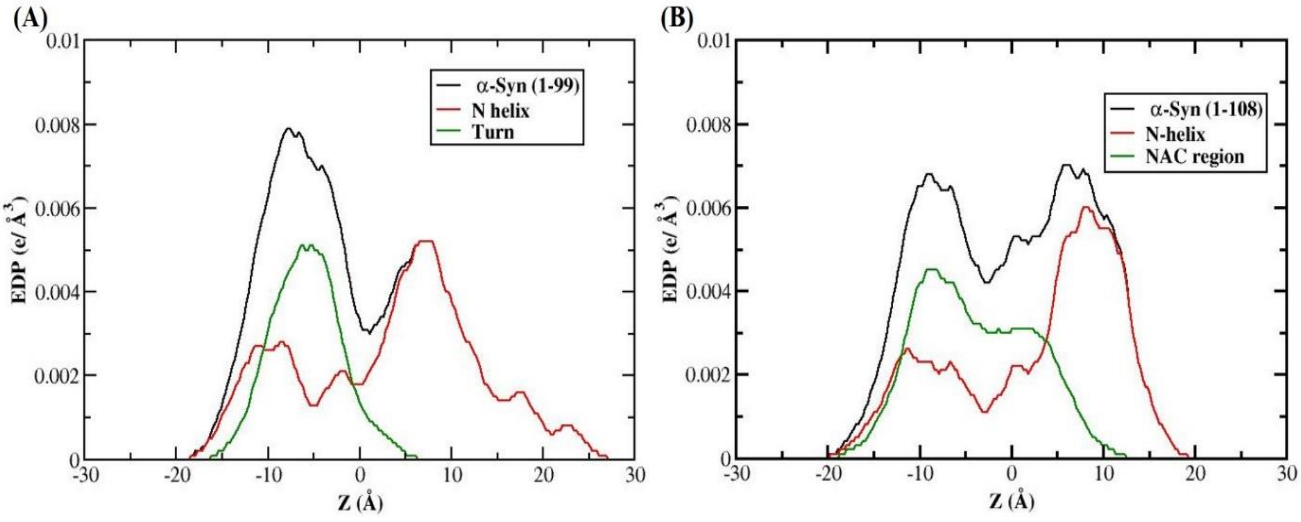

***Figure 9.4**. Electron Density Profile analysis of each region of truncated CTD α-Syn (A) (1-99) and (B) (1-108) from the MD simulation trajectories of 100 ns*

9.4.3. RMSD analysis:

The RMSD of the truncated CTD α-Syn (1-99 and 1-108) relative to the initial structure were calculated to monitor the convergence of systems (as shown in **Figure 9.5**). From the RMSD analysis, both the truncated CTD α-Syn (1-99 and 1-108) systems have been found to be stable.

But among the two systems, less truncated CTD α-Syn (1-108) showed more stability than more truncated CTD α-Syn (1-99). The overall structural RMSD analysis of α-Syn (1-108) monomer showed oscillation until 40 ns and then reached convergence around 4.8 Å. However, the RMSD value of α-Syn (1-99) was fluctuating initially and was found to converge around 6 Å after 55 ns of the simulation. Also, the RMSD profile for N-terminal and NAC regions was analyzed for both the α-Syn (1-99 and 1-108) monomers and was observed to have higher stability in the case of truncated CTD α-Syn (1-108) as shown in **Figure 9.6**. Therefore, the truncated CTD α-Syn (1-108) monomer was observed to be comparatively more stable than the truncated CTD α-Syn (1-99) monomer.

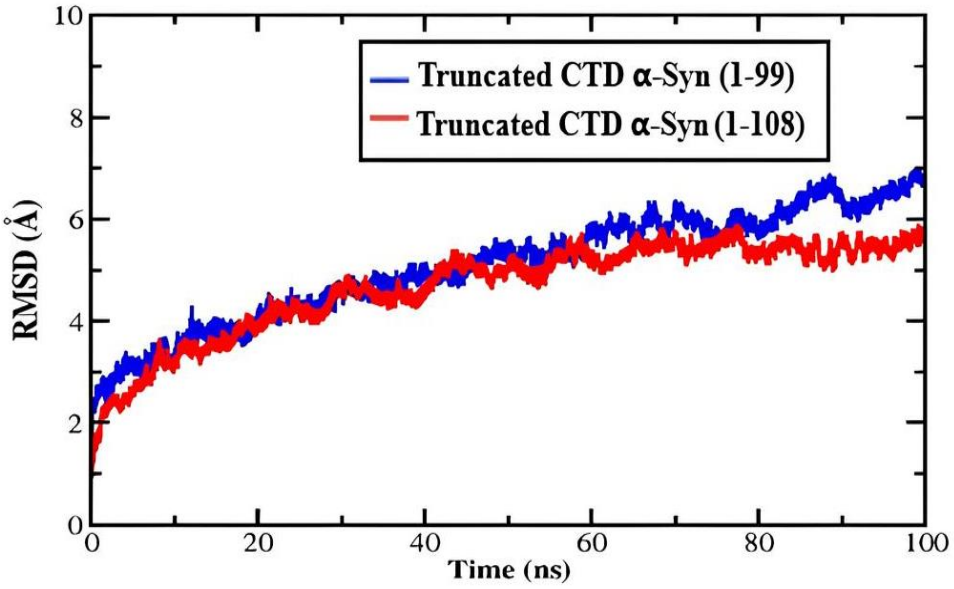

***Figure 9.5**. RMSD analysis of all the Cα atoms of truncated CTD α-Syn (A) (1-99) and (B) (1-108) from the MD simulation trajectories of 100 ns*

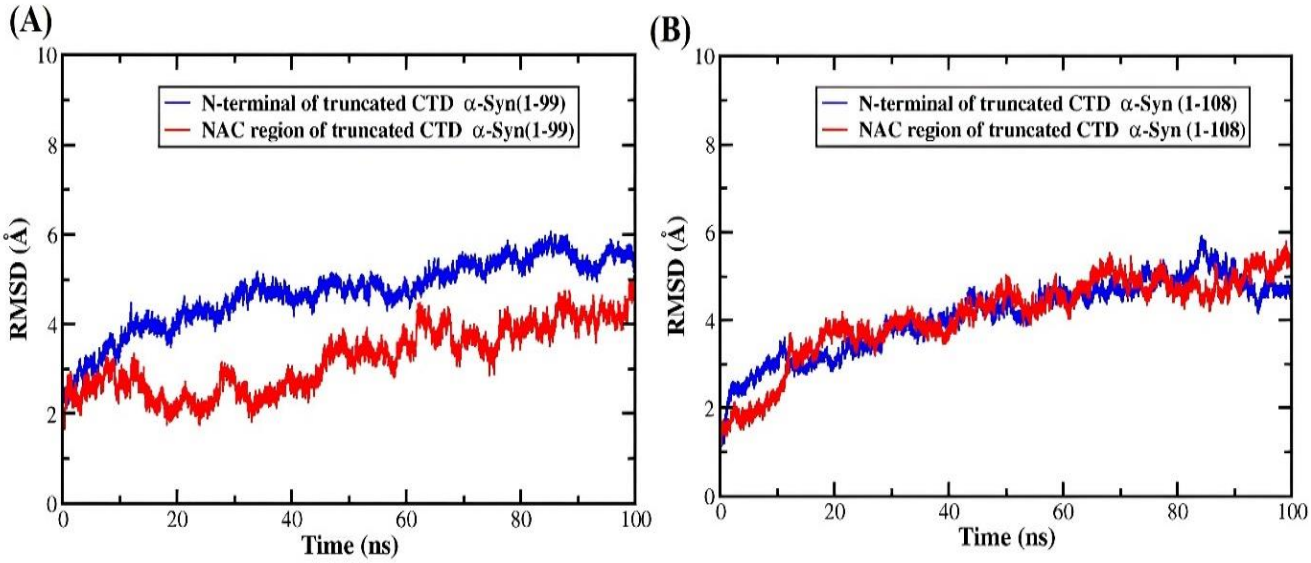

***Figure 9.6**. RMSD analysis of N-terminal and NAC region of truncated CTD α-Syn (A) (1-99) and (B) (1-108) from the MD simulation trajectories of 100 ns*

9.4.4. RMSF analysis:

The RMSF measures the average deviation of a truncated CTD α-Syn (1-99 and 1-108) over time from the time-averaged position of the particle. Thus, RMSF analyses the portions of the structure that are fluctuating from their equilibrium positions. The N-terminal and NAC region of both the truncated CTD α-Syn (1-99 and 1-108) were quite flexible throughout the MD simulation as shown in **Figure 9.7.** From the RMSF analysis, the NAC region was found to be more flexible than the N-terminal regions in both the truncated CTD α-Syn (1-99 and 1-108) monomers.

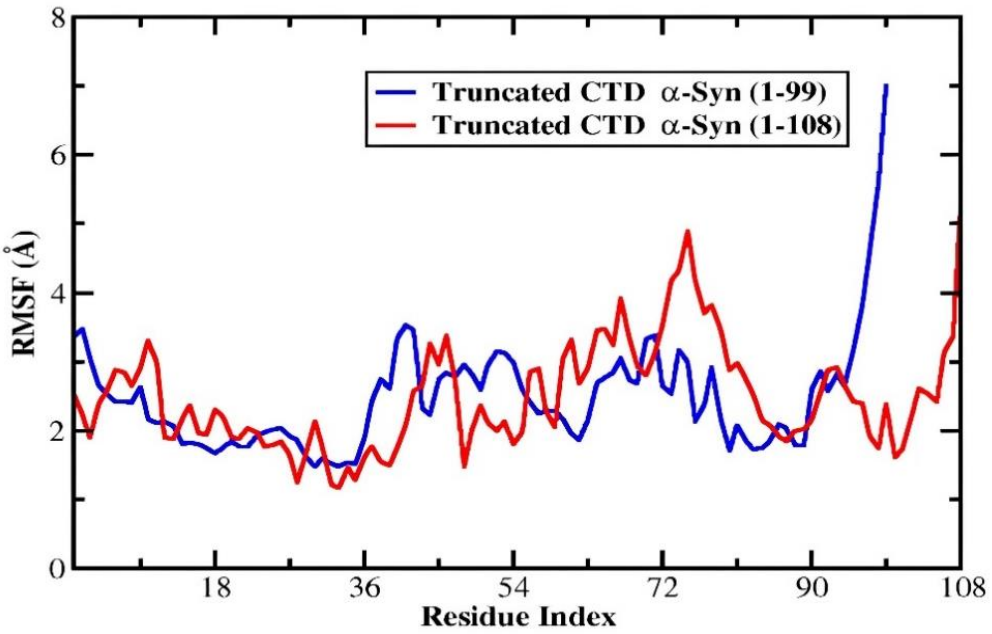

***Figure 9.7**. RMSF analysis of all the Cα atoms of truncated CTD α-Syn (A) (1-99) and (1-108) from the MD simulation trajectories of 100 ns*

9.4.5. Secondary Structural Analysis:

Protein structural stability was determined by time-dependent secondary structure analysis. The DSSP technique was used to analyze secondary structural changes during MD simulation of 100 ns [295] were observed in **Figure 9.8**. RMSF plots showed that protein flexibility from its N-terminal to its C-terminal was linked to secondary structure content. Truncated CTD α-Syn (1-99) and (1-108) were closely studied to learn how truncation affects secondary structure and leads to more stable structures. The N-terminal and NAC regions of truncated CTD α-Syn (1–99) and (1–108) showed significant probable secondary structural alterations (**Figure 9.9**).

The proportion of secondary structural content in truncated CTD α-Syn (1-99) and (1-108) was calculated using SOPMA software and results were tabulated in **Table 9.1** [286]. From **Table 9.1**, it was observed that the truncated CTD α-Syn (1-99) have a higher percentage of α-helices and extended strands while coil content and β-turn strands are higher in α-Syn (1-108). From the previous study, secondary structural content of untruncated α-Syn showed to have lower α-helical content alongwith higher coils and β-turn strands as compared to truncated CTD α-Syn (1-99 and 1-108) [547]. Similar findings were observed related to secondary structural content from our previous study [583].

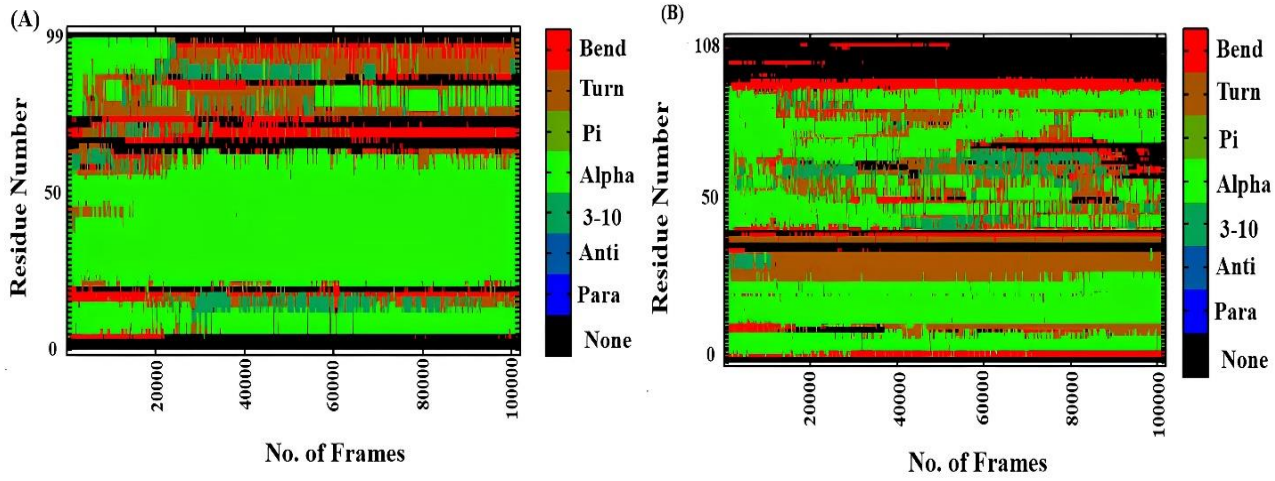

***Figure 9.8**. DSSP plot of secondary Structural content of truncated CTD α-Syn (A) (1-99) and (B) (1-108) during MD simulation obtained from Kabsch and Sander algorithm*

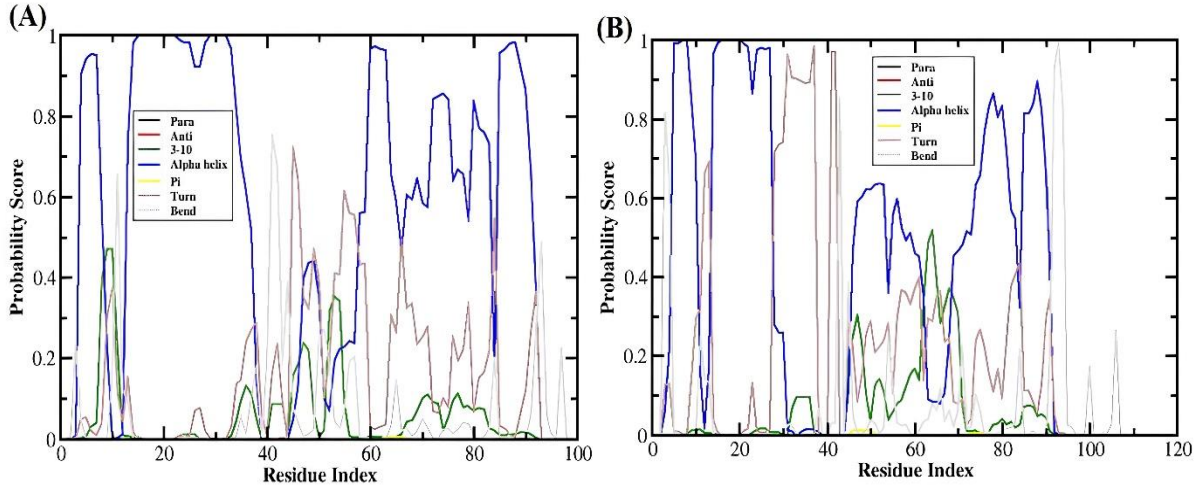

***Figure 9.9.** Secondary structure Probability Score of N-terminal and NAC region of truncated CTD α-Syn (A) (1-99) and (B) (1-108) from the MD simulation trajectories of 100 ns*

***Table 9.1.** Secondary Structural details of the truncated CTD α-Syn showing the percentage of secondary contents and similarity threshold as predicted by SOPMA*

Secondary structures	Truncated CTD α-Syn (1-99) (%)	Truncated CTD α-Syn (1-108) (%)
α-helix	77.78	69.44
β-turn	7.07	8.33
Coil	8.08	15.81
Extended strand	7.07	6.41

9.4.6. Radius of gyration analysis:

The mass-weighted root mean square distance of a collection of atoms from the shared center of mass is known as the radius of gyration (Rg). The radius of gyration provided an observation into a dimension of the truncated CTD α-Syn monomers (1-99 and 1-108) through the MD simulation trajectories of 100 ns. The radius of gyration plot for Cα atoms of truncated CTD α-Syn monomers (1-99 and 1-108) was shown in **Figure 9.10.** The Rg value was found to be in the range of 22.8-26.5Å and 29.4- 31.4 Å for truncated CTD α-Syn (1-99) and α-Syn (1-108), respectively. The trend of variations of Rg values showed that the orientation of truncated CTD α-Syn had a noticeable difference between the α-Syn (1-99 and 1-108) monomers. From the analysis, the value observed suggested that the α-Syn (1-99) monomer showed higher compactness than α-Syn (1-108).

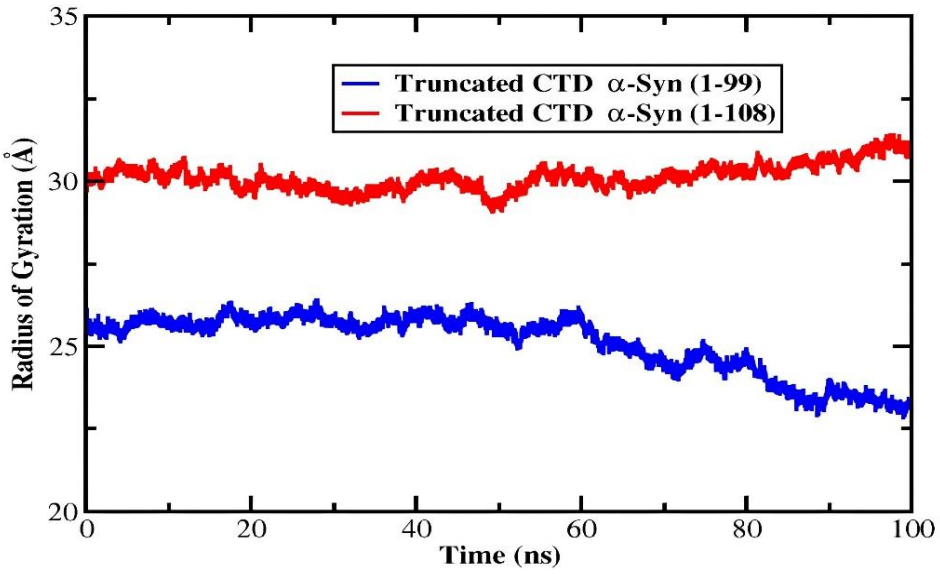

***Figure 9.10**. Radius of gyration analysis of truncated CTD α-Syn (A) (1-99) and (B) (1-108) from the MD simulation trajectories of 100 ns*

9.4.7. Hydrogen bond analysis between membrane and NAC region of CTD α-Synuclein monomers:

The proximity between the NAC regions of CTD α-Syn (1-99 and 1-108) monomers and lipid membrane were determined as shown in **Figure 9.11**. The number of hydrogen bonds formed between the NAC region and the membrane was found to be higher in the α-Syn (1-108) than in α-Syn (1-99). The list of number of hydrogen bonds between lipid membrane NAC region of CTD α-Syn (1-99 and 1-108) monomers that act as an acceptor or donor were tabulated in **Tables 9.2-9.5**. The strong interaction between the NAC regions of CTD α-Syn (1-108) was evident as the structural dynamics of α-Syn showed a higher coiled conformation as a result the N-terminal and NAC region is in close proximity that stabilizes the structure and ensures stronger interaction of the NAC region of α-Syn (1-108) with the membrane than α-Syn (1-99) monomer.

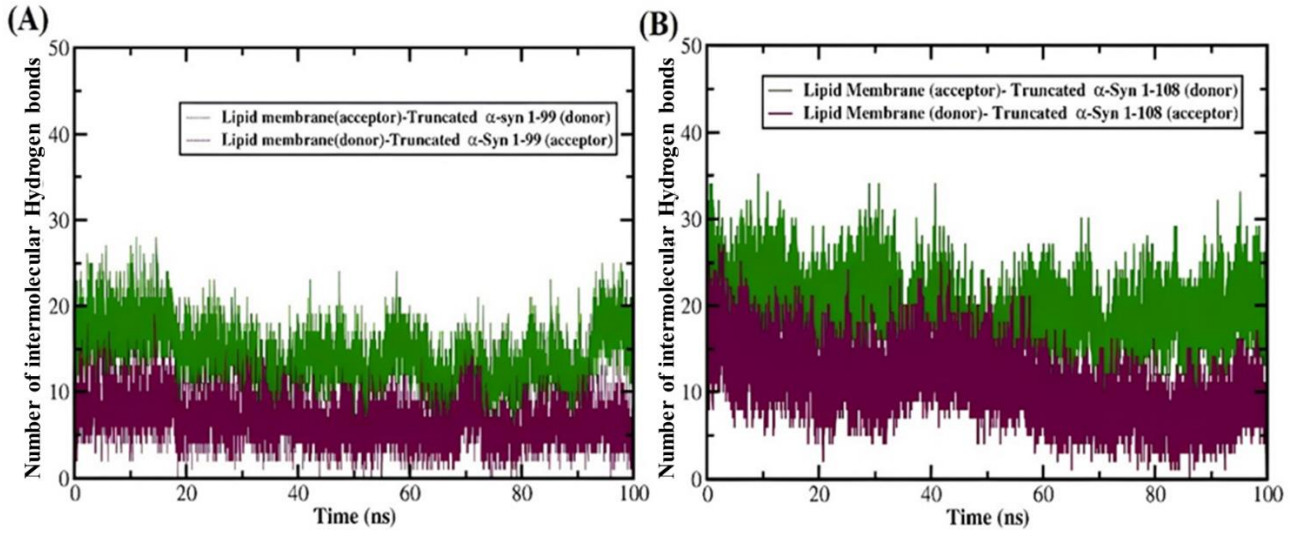

***Figure 9.11**. Intermolecular hydrogen bond analysis between the NAC region of truncated CTD α-Syn (A) (1-99) and (B) (1-108) and Lipid membrane from the MD simulation trajectories of 100 ns*

***Table 9.2.** Intermolecular Hydrogen bond analysis of membrane-bound truncated CTD α-Syn (1-99) during the MD simulation of 100 ns with membrane bilayer as acceptor and truncated CTD α-Syn (1-99) as donor*

#Acceptor	DonorH	Donor	Average Distance (Å)	Average Angle (º)
PS_1805@O22	SER_42@HG	SER_42@OG	2.6459	162.7636
PE_1757@O22	THR_33@HG1	THR_33@OG1	2.7286	160.2631
PE_1793@O22	LYS_21@HZ2	LYS_21@NZ	2.7864	156.9864
PC_1796@O12	LYS_21@HZ3	LYS_21@NZ	2.7858	159.2763
PC_1796@O22	GLN_24@HE22	GLN_24@NE2	2.865	157.2654
PE_1757@O34	LYS_32@HZ3	LYS_32@NZ	2.7171	157.9988

PE_1757@O12	GLY_36@H	GLY_36@N	2.8785	158.912
PE_1757@O12	LYS_34@H	LYS_34@N	2.8507	149.4409
PE_1757@O34	LYS_32@HZ1	LYS_32@NZ	2.7461	158.8526
PC_1796@O12	LYS_21@HZ1	LYS_21@NZ	2.7929	161.4462
PE_1793@O22	LYS_21@HZ3	LYS_21@NZ	2.7693	154.3011
PE_1757@HS	THR_33@HA	THR_33@CA	2.9206	143.8614
PS_1769@O34	LYS_45@HZ2	LYS_45@NZ	2.7543	158.9133
PC_1796@O12	LYS_21@HZ2	LYS_21@NZ	2.7829	159.6961
PE_1859@O34	LYS_12@HZ3	LYS_12@NZ	2.7446	158.2162
PE_1757@O34	LYS_32@HZ2	LYS_32@NZ	2.7583	158.5037
PE_1793@O22	LYS_21@HZ1	LYS_21@NZ	2.7697	153.1979
PE_1823@O12	LYS_43@HZ2	LYS_43@NZ	2.7643	153.616
PS_1805@O12	LYS_43@HZ3	LYS_43@NZ	2.785	157.1619
PE_1859@O34	LYS_12@HZ2	LYS_12@NZ	2.7614	158.9959
PS_1805@O12	LYS_43@HZ1	LYS_43@NZ	2.7893	156.0393
PE_1823@O12	LYS_43@HZ1	LYS_43@NZ	2.7676	154.7762
PS_1814@O36	LYS_6@HZ1	LYS_6@NZ	2.755	159.5243
PE_1823@O12	LYS_43@HZ3	LYS_43@NZ	2.7624	153.8809
PS_1769@O34	LYS_45@HZ3	LYS_45@NZ	2.7541	158.2905
PS_1769@O34	LYS_45@HZ1	LYS_45@NZ	2.7555	157.8602
PS_1814@O33	LYS_6@HZ1	LYS_6@NZ	2.7693	158.006
PS_1805@O36	LYS_43@HZ2	LYS_43@NZ	2.7369	155.9447
PS_1814@O36	LYS_6@HZ2	LYS_6@NZ	2.7721	155.4074
PE_1766@O12	GLY_41@H	GLY_41@N	2.8251	161.7058
PS_1805@O12	LYS_43@HZ2	LYS_43@NZ	2.7753	155.3097
PE_1757@O22	LYS_32@HZ2	LYS_32@NZ	2.7836	160.8538
PS_1814@O33	LYS_6@HZ3	LYS_6@NZ	2.7942	158.0796
PS_1814@O33	LYS_6@HZ2	LYS_6@NZ	2.7779	157.565
PE_1784@O33	LYS_10@HZ3	LYS_10@NZ	2.7603	156.5691
PS_1769@O12	LYS_45@HZ3	LYS_45@NZ	2.811	151.8662
OL_1773@H5S	LYS_21@HE2	LYS_21@CE	2.8933	151.1951
PC_1796@O22	LYS_21@HZ3	LYS_21@NZ	2.7404	148.2704
PE_1784@O33	LYS_10@HZ2	LYS_10@NZ	2.7686	158.1176
PS_1805@O36	LYS_43@HZ3	LYS_43@NZ	2.7353	156.2588
PS_1805@O36	LYS_43@HZ1	LYS_43@NZ	2.7363	155.7171
PE_1811@O33	LYS_10@HZ3	LYS_10@NZ	2.7512	156.3612
PS_1814@O35	LYS_6@HZ2	LYS_6@NZ	2.7946	156.0532
PE_1829@O12	SER_42@HG	SER_42@OG	2.6587	161.226
PS_1805@O35	LYS_43@HZ2	LYS_43@NZ	2.7264	155.833
PC_1739@O22	LYS_45@HZ1	LYS_45@NZ	2.7637	151.8223
PC_1739@O22	LYS_45@HZ3	LYS_45@NZ	2.7557	151.0537
PS_1805@O35	LYS_43@HZ3	LYS_43@NZ	2.7239	155.9514
PS_1814@O36	LYS_6@HZ3	LYS_6@NZ	2.7695	156.8093
PS_1805@O35	LYS_43@HZ1	LYS_43@NZ	2.7122	157.5985

Table 9.3. *Intermolecular Hydrogen bond analysis of membrane bound truncated CTD α-Syn (1-99) during the MD simulation of 100 ns with membrane bilayer as donor and truncated CTD α-Syn (1-99) as acceptor*

#Acceptor	DonorH	Donor	Average Distance (Å)	Average Angle (º)
THR_33@HA	PE_1757@HS	PE_1757@C1	2.9278	145.7881
THR_59@OG1	PE_1793@HN1C	PE_1793@N31	2.8512	156.7919
LYS_21@HZ3	PC_1796@HS	PC_1796@C1	2.9169	144.3737
LYS_21@HE2	OL_1773@H5S	OL_1773@C15	2.8928	152.9466
THR_59@OG1	PE_1793@HN1A	PE_1793@N31	2.8422	150.9139
SER_42@O	PE_1907@HN1B	PE_1907@N31	2.8113	151.606
GLY_41@O	PE_1766@HN1A	PE_1766@N31	2.8094	150.1653
TYR_39@HA	OL_1822@H8R	OL_1822@C18	2.9237	144.3823
GLY_41@O	PE_1766@HN1C	PE_1766@N31	2.8148	152.0944
GLY_41@O	PE_1766@HN1B	PE_1766@N31	2.8189	151.4807
ALA_18@HA	OL_1773@H10R	OL_1773@C110	2.8724	144.9962
LYS_21@HB2	OL_1858@H10R	OL_1858@C110	2.9115	145.5904
GLY_36@H	OL_1756@H3S	OL_1756@C13	2.8481	151.0635
LYS_21@HE3	OL_1771@H2S	OL_1771@C12	2.8841	142.7765
LYS_21@HE3	OL_1771@H2R	OL_1771@C12	2.9039	152.5515
GLY_36@HA3	OL_1756@H2R	OL_1756@C12	2.9303	144.0432
LYS_43@HE3	OL_1822@H4R	OL_1822@C14	2.9027	147.5866
VAL_3@O	PE_1811@HN1A	PE_1811@N31	2.7983	147.4208
VAL_3@O	PE_1811@HN1C	PE_1811@N31	2.8107	150.7436
SER_42@O	PE_1907@HN1C	PE_1907@N31	2.8139	150.0918
LYS_32@HA	OL_1822@H4S	OL_1822@C14	2.9105	140.7996
LYS_32@HD3	OL_1792@H9R	OL_1792@C19	2.9059	146.47
LEU_38@HG	OL_1822@H9R	OL_1822@C19	2.9122	144.6613
LYS_32@HE3	PE_1757@HX	PE_1757@C2	2.8741	145.3991
LYS_34@HE3	OL_1822@H5R	OL_1822@C15	2.8947	145.7069
VAL_3@O	PE_1811@HN1B	PE_1811@N31	2.8123	150.8338
LYS_21@HZ2	PC_1796@HS	PC_1796@C1	2.918	148.5435
VAL_3@H	OL_1857@H4R	OL_1857@C14	2.8684	156.6537
THR_22@HB	OL_133@H10R	OL_133@C110	2.8918	145.3123
LYS_34@HE3	OL_1822@H7S	OL_1822@C17	2.9086	147.6524
THR_22@HA	OL_1773@H14S	OL_1773@C114	2.927	144.1751
GLY_36@HA3	OL_1756@H3S	OL_1756@C13	2.925	144.9267
ALA_17@HA	OL_1858@H9R	OL_1858@C19	2.8892	147.3495
LYS_32@HG2	PE_1757@HX	PE_1757@C2	2.9381	141.6643
LYS_21@HE3	OL_1773@H3R	OL_1773@C13	2.8961	147.103
TYR_39@HA	OL_1822@H9R	OL_1822@C19	2.8672	142.0265
LYS_21@HE3	OL_1794@H3S	OL_1794@C13	2.9049	149.999
LYS_21@HZ1	PC_1796@HS	PC_1796@C1	2.9283	145.7649
GLY_25@HA2	OL_1794@H8S	OL_1794@C18	2.9262	143.1783

THR_59@OG1	PE_1793@HN1B	PE_1793@N31	2.8241	153.0022
LYS_21@HE2	OL_1771@H2R	OL_1771@C12	2.9158	145.6806
LYS_21@HE2	OL_1773@H4R	OL_1773@C14	2.8901	146.3354
LYS_32@HB2	OL_1824@H9R	OL_1824@C19	2.9192	148.8334
LYS_21@HA	OL_1858@H14R	OL_1858@C114	2.9423	145.2805
LYS_34@HE3	OL_1822@H6R	OL_1822@C16	2.8906	146.2884
LYS_43@HE2	OL_1804@H2S	OL_1804@C12	2.9036	143.7149
LYS_21@HE3	OL_1773@H4R	OL_1773@C14	2.8905	145.2512

Table 9.4. *Intermolecular Hydrogen bond analysis of membrane bound truncated CTD α-Syn (1-108) during the MD simulation of 100 ns with membrane bilayer as acceptor and truncated CTD α-Syn (1-108) as donor*

#Acceptor	DonorH	Donor	Average Distance (Å)	Average Angle (º)
PS_1805@O22	SER_42@HG	SER_42@OG	2.6459	162.7636
PS_1760@O12	GLY_101@H	GLY_101@N	2.8383	160.72
PE_1757@O22	THR_33@HG1	THR_33@OG1	2.7286	160.2631
PE_1793@O22	LYS_21@HZ2	LYS_21@NZ	2.7864	156.9864
PC_1796@O12	LYS_21@HZ3	LYS_21@NZ	2.7858	159.2763
PC_1796@O22	GLN_24@HE22	GLN_24@NE2	2.865	157.2654
PE_1856@O12	SER_87@HG	SER_87@OG	2.6751	159.484
PE_1757@O34	LYS_32@HZ3	LYS_32@NZ	2.7171	157.9988
PE_1856@O22	SER_87@HG	SER_87@OG	2.6475	164.2546
PE_1802@O33	LYS_80@HZ3	LYS_80@NZ	2.7594	158.3673
PE_1757@O12	GLY_36@H	GLY_36@N	2.8785	158.912
PE_1757@O12	LYS_34@H	LYS_34@N	2.8507	149.4409
PE_1748@O22	LYS_96@H	LYS_96@N	2.8331	160.2151
PE_1802@O33	LYS_80@HZ2	LYS_80@NZ	2.7556	158.1564
PE_1733@O34	LYS_102@HZ1	LYS_102@NZ	2.7645	158.7068
PE_1757@O34	LYS_32@HZ1	LYS_32@NZ	2.7461	158.8526
PE_1748@O34	LYS_96@HZ3	LYS_96@NZ	2.7475	159.629
PE_1802@O33	LYS_80@HZ1	LYS_80@NZ	2.7639	158.3818
PC_1796@O12	LYS_21@HZ1	LYS_21@NZ	2.7929	161.4462
PE_1748@O34	LYS_96@HZ2	LYS_96@NZ	2.764	158.8901
PE_1733@O34	LYS_102@HZ2	LYS_102@NZ	2.769	158.5764
PE_1793@O22	LYS_21@HZ3	LYS_21@NZ	2.7693	154.3011
PE_1757@HS	THR_33@HA	THR_33@CA	2.9206	143.8614
PS_1769@O34	LYS_45@HZ2	LYS_45@NZ	2.7543	158.9133
PS_1781@O22	LEU_100@H	LEU_100@N	2.8639	158.9773
PC_1796@O12	LYS_21@HZ2	LYS_21@NZ	2.7829	159.6961
PS_1781@O34	LYS_102@HZ2	LYS_102@NZ	2.751	158.2091
PE_1859@O34	LYS_12@HZ3	LYS_12@NZ	2.7446	158.2162
PE_1757@O34	LYS_32@HZ2	LYS_32@NZ	2.7583	158.5037
PE_1802@O22	LYS_80@HZ2	LYS_80@NZ	2.7843	155.7155

PS_1742@O32	GLU_105@H	GLU_105@N	2.8926	160.4128
PE_1733@O34	LYS_102@HZ3	LYS_102@NZ	2.7721	157.93
PS_1781@O34	LYS_102@HZ3	LYS_102@NZ	2.753	158.7438
PE_1748@O34	LYS_96@HZ1	LYS_96@NZ	2.756	158.7633
PE_1793@O22	LYS_21@HZ1	LYS_21@NZ	2.7697	153.1979
PE_1823@O12	LYS_43@HZ2	LYS_43@NZ	2.7643	153.616
PS_1805@O12	LYS_43@HZ3	LYS_43@NZ	2.785	157.1619
PE_1859@O34	LYS_12@HZ2	LYS_12@NZ	2.7614	158.9959
PS_1805@O12	LYS_43@HZ1	LYS_43@NZ	2.7893	156.0393
PS_1781@O34	LYS_102@HZ1	LYS_102@NZ	2.7845	159.9598
PE_1802@O22	LYS_80@HZ3	LYS_80@NZ	2.7772	156.3604
PS_1781@O35	LYS_97@H	LYS_97@N	2.8328	163.9931
PE_1823@O12	LYS_43@HZ1	LYS_43@NZ	2.7676	154.7762
PE_1808@O12	GLY_93@H	GLY_93@N	2.8382	159.9763
PS_1814@O36	LYS_6@HZ1	LYS_6@NZ	2.755	159.5243
PE_1802@O22	LYS_80@HZ1	LYS_80@NZ	2.7799	157.0774
PE_1823@O12	LYS_43@HZ3	LYS_43@NZ	2.7624	153.8809
PS_1769@O34	LYS_45@HZ3	LYS_45@NZ	2.7541	158.2905
PS_1769@O34	LYS_45@HZ1	LYS_45@NZ	2.7555	157.8602
PS_1763@O33	GLY_106@H	GLY_106@N	2.8459	160.0748
PS_1760@HR	GLY_101@HA3	GLY_101@CA	2.9259	142.1667

Table 9.5. *Intermolecular Hydrogen bond analysis of membrane bound truncated CTD α-Syn (1-108) during the MD simulation of 100 ns with membrane bilayer as donor and truncated CTD α-Syn (1-108) as acceptor*

#Acceptor	DonorH	Donor	Average Distance (Å)	Average Angle (º)
THR_33@HA	PE_1757@HS	PE_1757@C1	2.9278	145.7881
THR_59@OG1	PE_1793@HN1C	PE_1793@N31	2.8512	156.7919
LYS_21@HZ3	PC_1796@HS	PC_1796@C1	2.9169	144.3737
LYS_21@HE2	OL_1773@H5S	OL_1773@C15	2.8928	152.9466
THR_59@OG1	PE_1793@HN1A	PE_1793@N31	2.8422	150.9139
SER_42@O	PE_1907@HN1B	PE_1907@N31	2.8113	151.606
GLY_41@O	PE_1766@HN1A	PE_1766@N31	2.8094	150.1653
TYR_39@HA	OL_1822@H8R	OL_1822@C18	2.9237	144.3823
GLY_41@O	PE_1766@HN1C	PE_1766@N31	2.8148	152.0944
GLY_41@O	PE_1766@HN1B	PE_1766@N31	2.8189	151.4807
ALA_18@HA	OL_1773@H10R	OL_1773@C110	2.8724	144.9962
LYS_21@HB2	OL_1858@H10R	OL_1858@C110	2.9115	145.5904
GLY_36@H	OL_1756@H3S	OL_1756@C13	2.8481	151.0635
LYS_21@HE3	OL_1771@H2S	OL_1771@C12	2.8841	142.7765
LYS_21@HE3	OL_1771@H2R	OL_1771@C12	2.9039	152.5515
GLY_36@HA3	OL_1756@H2R	OL_1756@C12	2.9303	144.0432
LYS_43@HE3	OL_1822@H4R	OL_1822@C14	2.9027	147.5866
VAL_3@O	PE_1811@HN1A	PE_1811@N31	2.7983	147.4208

VAL_3@O	PE_1811@HN1C	PE_1811@N31	2.8107	150.7436
SER_42@O	PE_1907@HN1C	PE_1907@N31	2.8139	150.0918
LYS_32@HA	OL_1822@H4S	OL_1822@C14	2.9105	140.7996
LYS_32@HD3	OL_1792@H9R	OL_1792@C19	2.9059	146.47
LEU_38@HG	OL_1822@H9R	OL_1822@C19	2.9122	144.6613
LYS_32@HE3 LYS_34@HE3	PE_1757@HX OL_1822@H5R	PE_1757@C2 OL_1822@C15	2.8741 2.8947	145.3991 145.7069
VAL_3@O	PE_1811@HN1B	PE_1811@N31	2.8123	150.8338
LYS_21@HZ2	PC_1796@HS	PC_1796@C1	2.918	148.5435
VAL_3@H	OL_1857@H4R	OL_1857@C14	2.8684	156.6537
THR_22@HB	OL_133@H10R	OL_133@C110	2.8918	145.3123
LYS_34@HE3	OL_1822@H7S	OL_1822@C17	2.9086	147.6524
THR_22@HA	OL_1773@H14S	OL_1773@C114	2.927	144.1751
GLY_36@HA3	OL_1756@H3S	OL_1756@C13	2.925	144.9267
ALA_17@HA	OL_1858@H9R	OL_1858@C19	2.8892	147.3495
LYS_32@HG2	PE_1757@HX	PE_1757@C2	2.9381	141.6643
LYS_21@HE3	OL_1773@H3R	OL_1773@C13	2.8961	147.103
TYR_39@HA	OL_1822@H9R	OL_1822@C19	2.8672	142.0265
LYS_21@HE3	OL_1794@H3S	OL_1794@C13	2.9049	149.999
LYS_21@HZ1	PC_1796@HS	PC_1796@C1	2.9283	145.7649
GLY_25@HA2	OL_1794@H8S	OL_1794@C18	2.9262	143.1783
THR_59@OG1	PE_1793@HN1B	PE_1793@N31	2.8241	153.0022
LYS_21@HE2	OL_1771@H2R	OL_1771@C12	2.9158	145.6806
LYS_21@HE2	OL_1773@H4R	OL_1773@C14	2.8901	146.3354
LYS_32@HB2	OL_1824@H9R	OL_1824@C19	2.9192	148.8334
LYS_21@HA	OL_1858@H14R	OL_1858@C114	2.9423	145.2805
LYS_34@HE3	OL_1822@H6R	OL_1822@C16	2.8906	146.2884
LYS_43@HE2	OL_1804@H2S	OL_1804@C12	2.9036	143.7149
LYS_21@HE3	OL_1773@H4R	OL_1773@C14	2.8905	145.2512
VAL_55@HG11	PE_1793@H2B	PE_1793@C32	2.8634	141.7919
SER_42@HB2	PS_1805@HX	PS_1805@C2	2.9461	145.4925
GLU_35@HB2	PE_1757@HR	PE_1757@C1	2.9553	142.7487

9.4.8. Principal Component Analysis (PCA):

The projection of the first two eigenvectors, containing the maximum motions, in conformational space for truncated CTD α-Syn (1-99 and 1-108), which identified the most stable structure. To examine the conformational structural changes, the Gibbs free energy landscape (FEL) was plotted against the first two principal components, namely PC1 and PC2, which describe the free energy of the protein that correlates with the 3-D arrangement of the molecule. **Figures 9.12** represent 2D and 3D plots of the FEL analysis and ΔG value of 0 to 3.5 kcal/mol for truncated CTD α-Syn (1-99 and 1-108) respectively. The global

energy minima conformations for truncated CTD α-Syn (1-99 and 1-108) were calculated to be less than 1.5 kcal/mol. The size and shape of the minimal energy area indicate the stability of the structure. Since the thermodynamically most stable structure resides in a minimum on the free-energy (ΔG) surface, more concentrated black areas suggest more stability of the corresponding structures during MD simulation. The CTD α-Syn (1-108) showed more concentrated minima (in 2D) and less dispersed basins (in the 3-D plot) as shown in **Figure 9.12(B)**, whereas the CTD α-Syn (1-108) displayed more dispersed regions (in the 3-D plot). The 2-D and 3-D plots of PCA demonstrated that the truncated CTD α-Syn (1-108) occupied lesser area in space and showed narrow variations in the conformational dynamics along the first two principal components, demonstrating its rigidity. On the contrary, truncated CTD α-Syn (1-99) was expanded in their conformational space due to their structural instability.

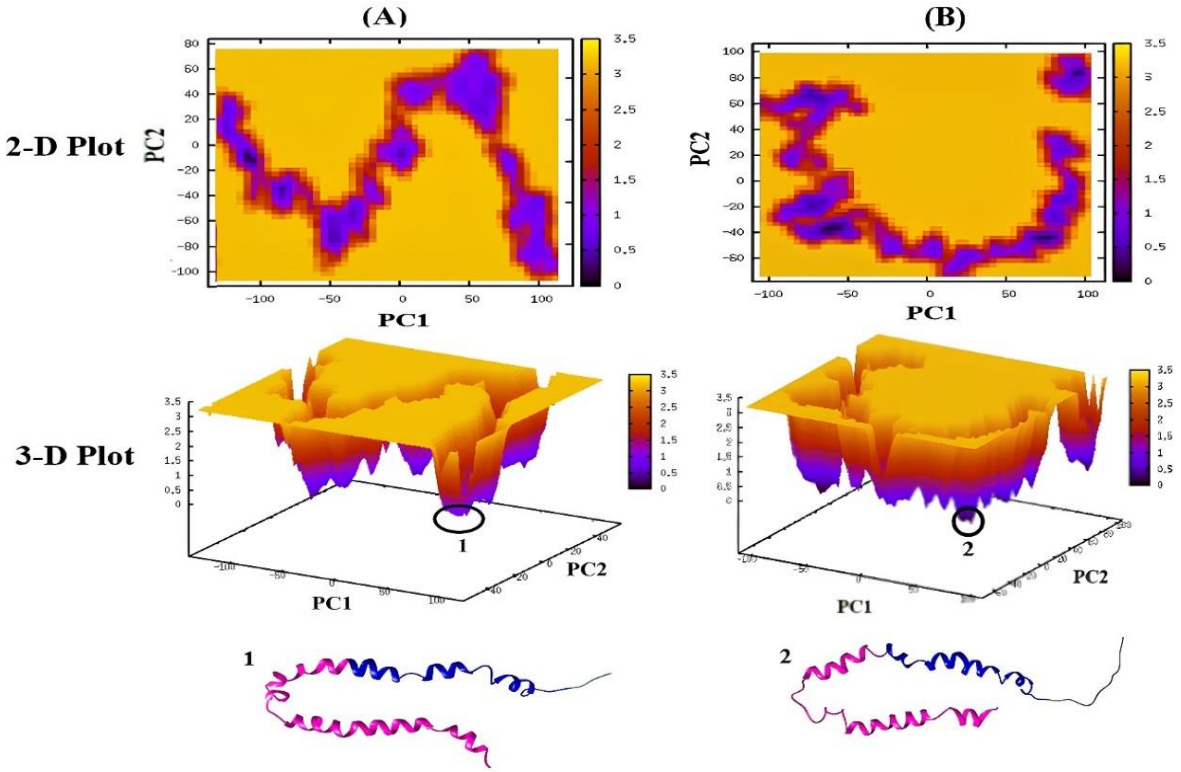

Figure 9.12. *Principle Component Analysis followed Gibbs free energy landscape (FEL) plot of truncated CTD α-Syn (A) (1-99) and (B) (1-108) from the MD simulation trajectories of 100 ns. (1) and (2) indicates lowest energy structure, along with the two principal eigenvectors (PC1 and PC2). The black region depicts conformations with lower energy, the red color signifies the meta-stable states and the blue corresponds to conformations having high energy*

9.4.9. Conformational Snapshots of truncated CTD (1-99 and 1-108) of α-Synuclein associated with membrane:

The conformational changes of the truncated CTD (1-99 and 1-108) of α-Syn monomers were observed from the MD trajectories as a function of simulation time. The conformational snapshots were obtained using UCSF Chimera [306] as shown in **Figure 9.13** and **Figure 9.14**. The average number of helices was observed to be relatively higher in the truncated CTD of α-Syn (1–99) monomer than in (1–108). Also, in the **Figure 9.14** the conformers of truncated CTD (1–108) of α-Syn monomer was observed to undergo folding due to an increase in the formation of secondary structures (β-sheets and coils). In comparison with the truncated α-Syn (1-99), the NAC region of untruncated α-Syn was observed to get elevated above the membrane surface and also the helix was found to be broken around the region (45-95). But, a slight elevation of the NAC region of CTD truncated (1-108) was observed during the MD simulation. The analysis of the untruncated α-Syn confirmed in our previous work that the nucleus of the α-Syn in water phase allows lipid unbound monomers to attract to the membrane that forms long, amyloid fibrils alongwith a cross β-sheet structure [547].Using the HELANAL server [285], the bending angles between two local helix axes, defined by four consecutive C_α atoms, were calculated and tabulated in **Table 9.6**. From **Table 9.6**, it was observed that the N-terminal of the α-Syn (1–99) monomer has a higher bending angle of 31.45º between helix axes (32K 35E 38L) that facilitates the N-terminal to undergo extended conformation, resulting in stronger interaction with the membrane surface as noticed in the conformational snapshots (**Figure 9.13**). On the contrary, the NAC region of the α-Syn (1-108) monomer was observed to have a higher bending angle of 47º between the helix axes (82V 85A 88I). Also, the length of the helix and the average number of helices per turn were also determined using the HELANAL server. A study noted that as the length of the helix rises, the bending of the monomers delays the stretching of the helices more. This suggests that short helices tend to stretch, whereas long helices tend to bend more [584].

Table 9.6. *Calculation of helix length, the bending angles between two local helix axes, and the average number of residues per turn of the truncated CTD (1-99) and (108) α-Syn using HELANAL server*

Complex	Helix (start→end)	Helix length	Average no. of residues per turn of the helix (n)	Bending angle (degrees)	Bending angle (residues)
Truncated CTD (1-99) α-Syn	4F-10K	7	3.39	31.45	32K 35E 38L
	13E-38L	26	3.34	24.76	72T 75T 78A
	66V-78A	13	3.56		
	85A-90A	6	3.54		

Truncated CTD (1-108) α-Syn	5M-9S	5	3.64	23.26	14G 17A 20E 82V 85A 88I
	14G-30A	17	3.57	47	
	55V-59T	5	3.54		
	74V-91A	18	3.57		

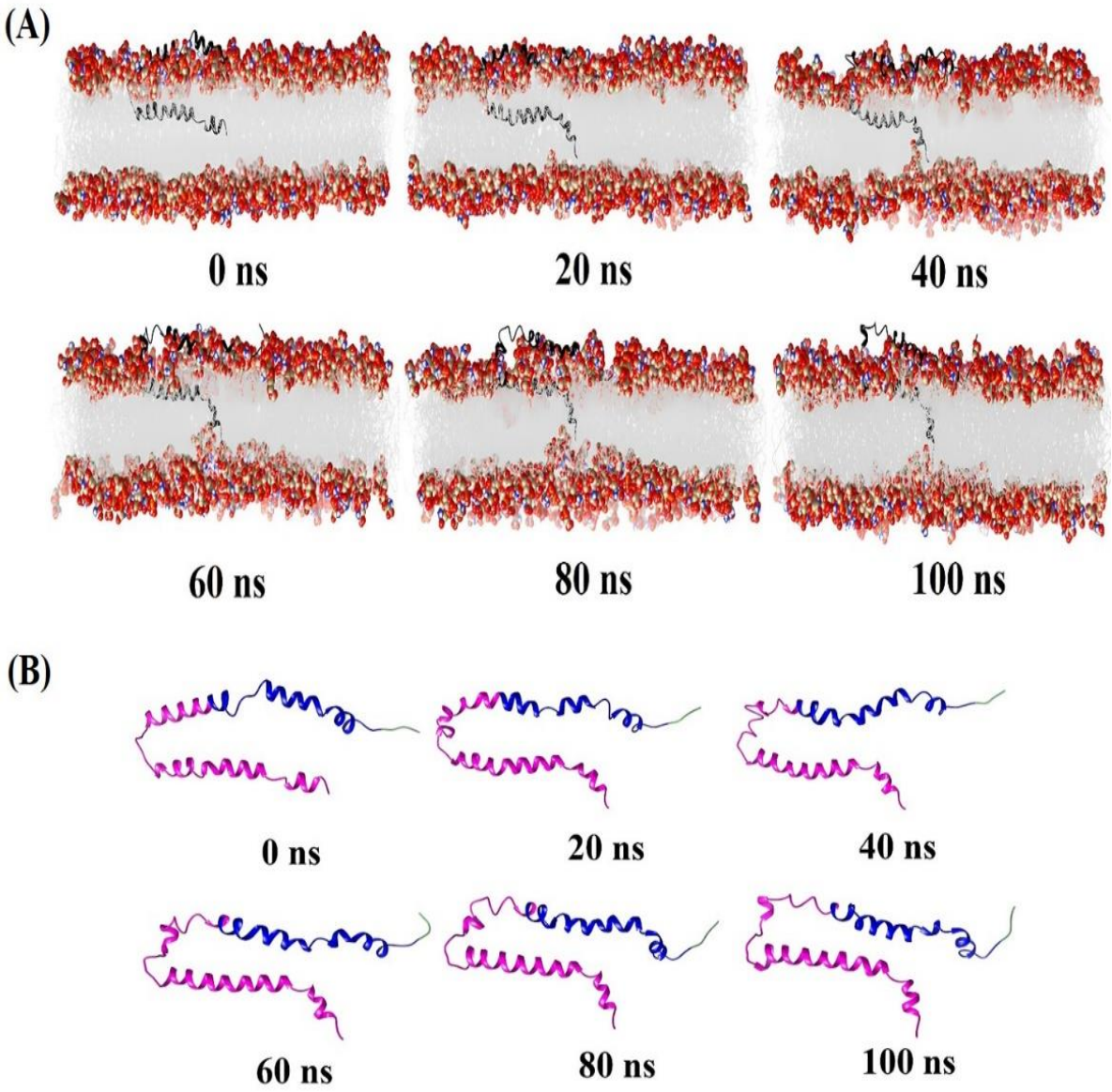

Figure 9.13. *Conformational snapshots of truncated CTD (1-99) (A) α-Syn in association with lipid membrane and (B) membrane hidden*

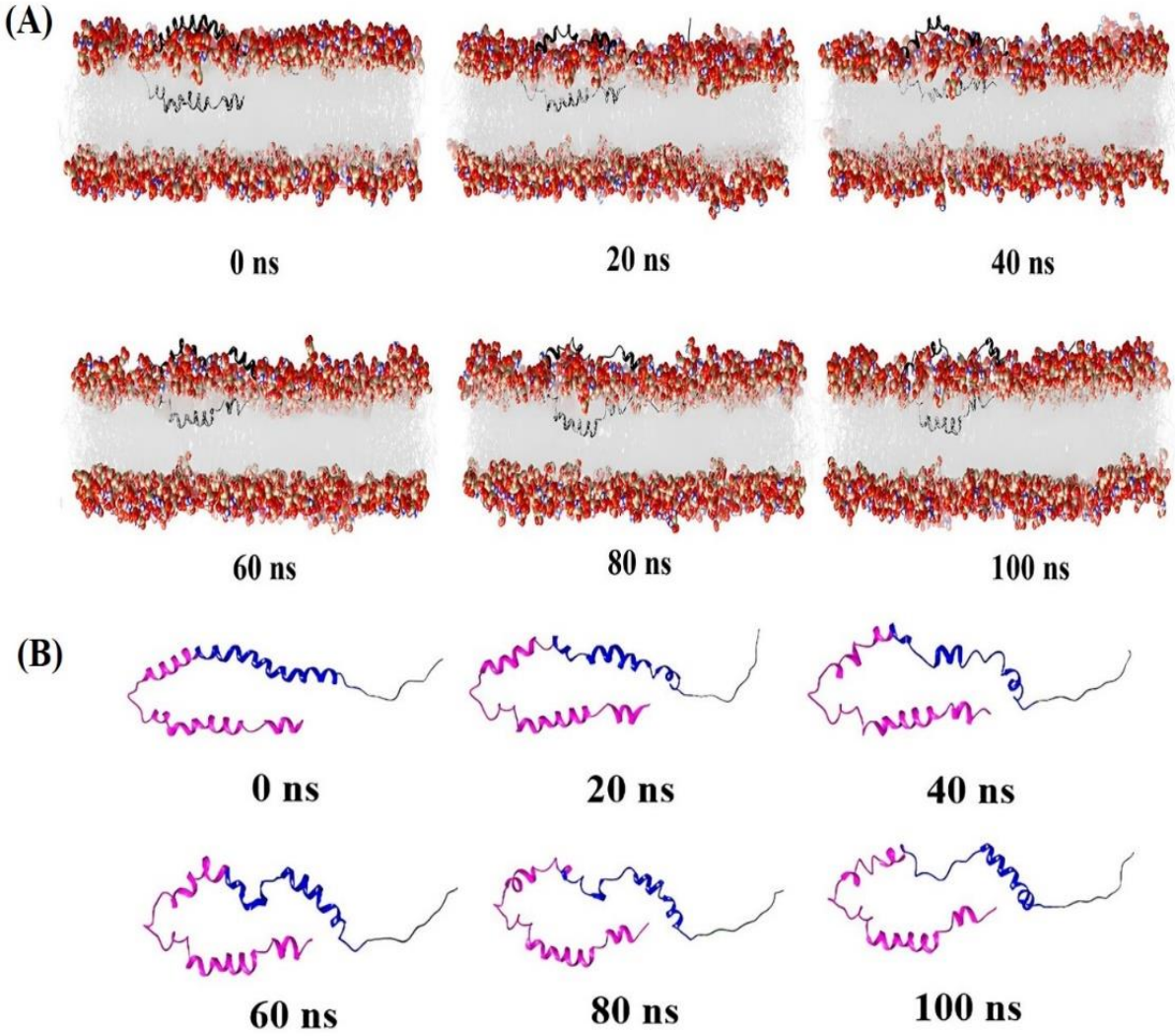

Figure 9.14. *Conformational snapshots of truncated CTD (1-108) (A) α-Syn in association with lipid membrane and (B) membrane hidden*

9.4.10. Distance Analysis:

The center of the mass distance between the N-terminal and C-terminal domains of truncated CTD α-Syn (1-99 and 1-108) monomers were analyzed as shown in **Figure 9.15**. From **Figure 9.15**, it was observed that the distance between the N-terminal and C-terminal domains for the truncated CTD α-Syn (1-108) was found to be lower than the α-Syn (1-99). However, the distance between the N-terminal and C-terminal domains for the truncated CTD α-Syn (1-108) was found to be more stable than the distance for the truncated CTD α-Syn (1-99).

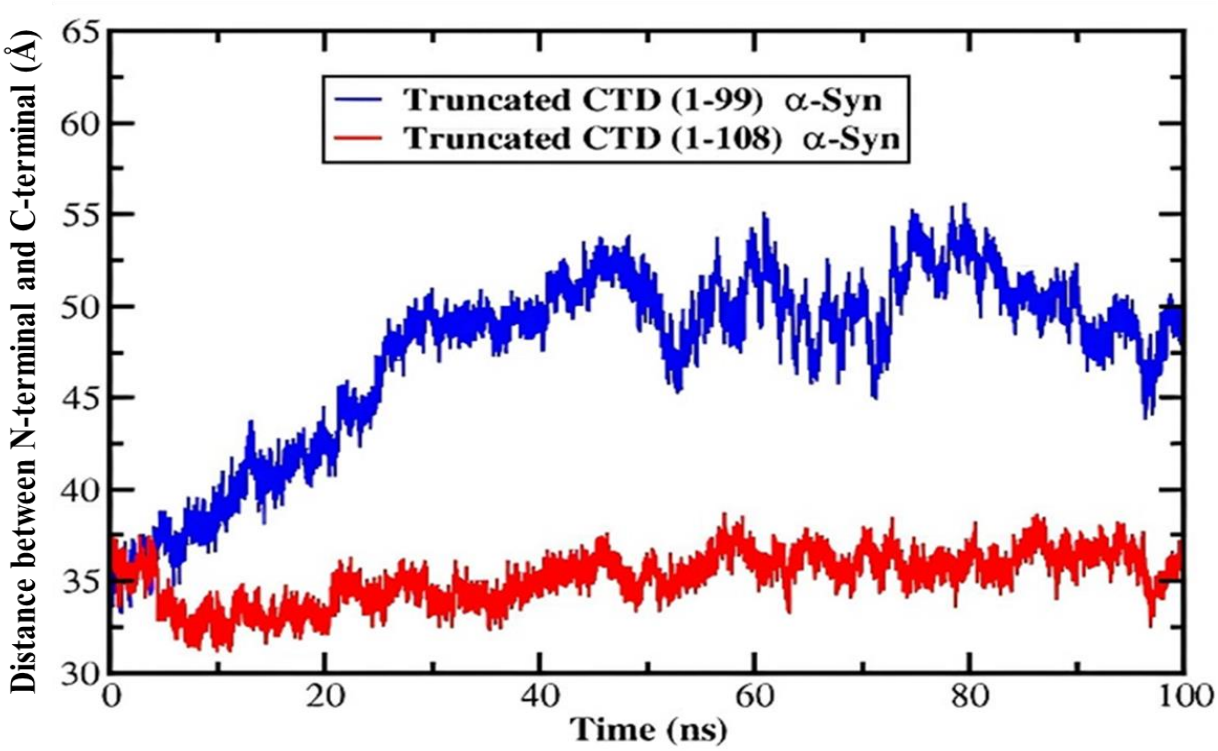

Figure 9.15. *Distance Analysis of truncated CTD α-Syn (1-99) and (1-108) from the MD simulation trajectories of 100 ns*

9.4.11. Salt Bridge interactions:

To ensure the stability of truncated CTD α-Syn (1-99) and (1-108), the number of salt bridges and their distance within the N-terminal, NAC, and C-terminal regions of the α-Syn were determined. The formation of salt bridges is one of the characteristics of the fibril, as are the various intramolecular interactions stabilizing the structure of α-Syn. Using the ESBRI server [259], the list of residue-residue interactions and the distance in (Å) within the N-terminal, NAC region, and C-terminal of the truncated CTD α-Syn (1-99) and (1-108) interface were evaluated and the results were summarized in **Table 9.7** and **Table 9.8**. From **Table 9.7** and **Table 9.8** it can be seen that a significant number of salt bridges were formed in the truncated CTD α-Syn (1-108) in comparison with α-Syn (1-99). From the ESBRI server analysis, it can be seen that a significant number of salt bridges were formed in the truncated CTD α-Syn (1-108) in comparison with α-Syn (1-99).

Table 9.7. *List of atom-atom interactions within the Truncated CTD α-Syn (1-99) interface from the ESBRI server*

α-Syn (1-99) (Residue 1)				Hydrogen Bonds	α-Syn (1-99) (Residue 2)				
Atom number	Atom name	Residue name	Residue number		Atom number	Atom name	Residue name	Residue number	Distance (Å)
124	NZ	LYS	6	<-->	118	OD1	ASP	2	1.68
124	NZ	LYS	6	<-->	119	OD2	ASP	2	0.50
120	NZ	LYS	23	<-->	120	OE1	GLU	20	2.86
114	NZ	LYS	43	<-->	108	OE1	GLU	35	1.63
118	NZ	LYS	58	<-->	119	OE1	GLU	61	2.81
115	NZ	LYS	60	<-->	114	OE1	GLU	57	2.87
118	NZ	LYS	80	<-->	119	OE1	GLU	83	3.11

Table 9.8. *List of atom-atom interactions within the Truncated CTD α-Syn (1-108) interface from the ESBRI server*

α-Syn (1-108) (Residue 1)				Hydrogen Bonds	α-Syn (1-108)(Residue 2)				
Atom number	Atom name	Residue name	Residue number		Atom number	Atom name	Residue name	Residue number	Distance (Å)
111	NZ	LYS	12	<-->	107	OE1	GLU	13	2.87
105	NZ	LYS	23	<-->	106	OE1	GLU	20	2.58
100	NZ	LYS	32	<-->	99	OE1	GLU	35	2.63
105	NZ	LYS	43	<-->	99	OE1	GLU	35	3.63
112	NZ	LYS	58	<-->	102	OE1	GLU	57	3.61
112	NZ	LYS	58	<-->	111	OE1	GLU	61	2.60
101	NZ	LYS	60	<-->	102	OE1	GLU	57	3.27
101	NZ	LYS	60	<-->	111	OE1	GLU	61	2.61
85	NZ	LYS	97	<-->	93	OD2	ASP	98	3.41

9.5. Conclusion:

In this study, using all-atom MD simulation, we have demonstrated the conformational dynamics of C-terminal truncated α-Syn (1-99 and 1-108) on its interaction with lipid membrane. The simulation studies including RMSD and RMSF profiles as a function of simulation time suggested that more truncation leads to instability and higher fluctuations of the α-Syn monomer. Also, the truncated CTD (1-108) α-Syn monomer showed lesser compactness than the truncated CTD (1-99) α-Syn as the monomeric form adopts different folding dynamics. The probable secondary structure of the truncated CTD α-Syn (1-99) monomer exhibits more extended helix conformation than the α-Syn (1-108) monomer. While in the truncated CTD α-Syn (1-99), coil conformations were observed to be higher. The conformational space of the truncated CTD -Syn (1-99) was increased due to the structural instability of the protein. The ΔG values obtained from free energy landscape analysis for truncated CTD α-Syn (1-99 and 1-108) were determined to be 0.35 kcal/mol. Additionally, the results showed that the conformational dynamics along the first two principal components showed limited variations. The conformational snapshots obtained from the MD trajectory as a function of the simulation time highlighted that the more truncated CTD α-Syn (1-99) monomer exhibited stronger interaction between the N-terminal and membrane lipid layer due to the formation of an extended strand. The CTD acts as a guard, controlling the α-Syn function. Truncation of the CTD enables the NAC domain to interact with other molecules of higher electrostatic potential [585]. Similarly, the inter-molecular hydrogen bond analysis between the NAC region of CTD α-Syn monomers and lipid membrane indicated stronger interaction in the case of lesser truncated CTD α-Syn (1-108). Our findings suggest that the truncation on the CTD of α-Syn affects its interaction with the membrane and subsequently has an impact on the aggregation.